Journal of Materials Chemistry C

Accepted Manuscript

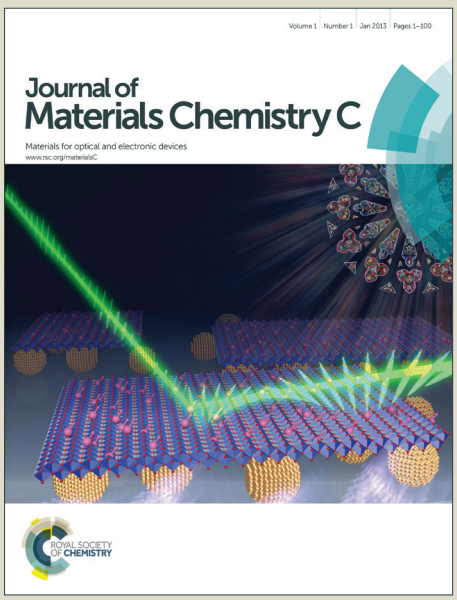

ROYAL SOCIETY OF CHEMISTRY

www.rsc.org/materialsC

Cite this: DOI: 10.1039/c0xx00000x

www.rsc.org/xxxxxx

ARTICLE TYPE

Unconventionally shaped chromonic liquid crystals formed by novel silver(I) complexes†§

Daniela Pucci,*[a] Barbara Sanz Mendiguchia,[a] Caterina Maria Tone,[b] Elisabeta Ildyko Szerb,[a] Federica Ciuchi,[c] Min Gao,[d] Mauro Ghedini[a] and Alessandra Crispini*[a]

Received (in XXX, XXX) XthXXXXXXXXX 20XX, Accepted Xth XXXXXXXXX 20XX
DOI: 10.1039/b000000x

The synthesis of the first chiral Ag(I) bis chelated bipypiridine ionic complexes showing chromonic liquid crystalline behaviour in water is reported. Single crystal X-ray analysis revealed a pre-chromonic organization in the crystalline state, with silver(I) cations stacking into columns reinforced by hydrogen bonding with the acetate counterions and water molecules. Due to the presence of molecules with an unconventional shape for the generation of typical chromonic phases, a full characterization based on phase diagram analysis, completely resolved by POM, DSC and X-Ray powder diffraction measurements, has been conducted. Moreover, cryo-TEM experiments have been carried out in order to confirm the appearance of the nematic columnar phases. A "route" to drive the alignment of the liquid crystalline phases of these compounds has been developed, particularly important for future application in biophotonic devices. Finally, the presence of transient twisted periodical stripe structures has been observed, when an initial planar alignment is destroyed in favour of a homeotropic configuration of the molecules dictated by the confining surfaces.

Introduction

Chromonics are a very interesting class of lyotropic liquid crystals (LLC), which have become in the last years, an important research topic in several domains, like optical materials and devices in high technology, molecular electronics and biological sensing.[1-3] Although the behaviour of these dynamic 'soft' phases is not completely understood yet, Lydon, Attwood and co-workers showed the main differences between the chromonic molecules and the conventional amphiphilic lyotropic liquid crystals.[1,4] The main structural features of the compounds forming this class of LLC is the lack of amphiphilic nature and the presence of a planar, aromatic π–delocalised core (with a disk-like shape), with solubilising groups (e.g. CO_2^-, SO_3^-) in the periphery of the molecules. In a polar solvent, molecules tend to aggregate into stacks due to weak intermolecular interactions, mainly van der Waals between the aromatic cores (π-π stacking), hydrophobic and electrostatic interactions. At all concentrations, there is some degree of aggregation and as the concentration increases, the distribution of the aggregates size shifts to higher and higher numbers of molecules. Therefore, instead of exhibiting a critical micellar concentration, these systems show isodesmic aggregation.[5] If the concentration is high enough to form large and interacting rod-like aggregates, liquid crystalline phases are formed. The stability of these phases depends on both temperature and concentration, and nematic phase, with just orientational order, together with columnar phase, with hexagonal packing, have been observed.[1,2] The majority of lyotropic chromonic liquid crystals (LCLCs) reported to date are based on organic system featuring the properties highlighted above. All these features, together with their ability to organize themselves into columns forming ordered phases and the possibility to align them between surfaces, make LCLCs ideal candidates for a new branch of application in photonic devices or biosening.[6]

Lately, some metal complexes have been shown to form LCLC phases.[7] Metal complexes have broad range of oxidation states and coordination geometries offering new opportunities for the design of original LCLC mesophases, rendering them advantageous over their organic counterparts.[8,9] Indeed, metal complexes may offer different functionalities, modulated by the type of coordinated ligands, as well as intriguing spectroscopic, catalytic and redox properties.

.The chemistry of Ag(I) complexes is in general extremely versatile in building supramolecular 'soft' ionic systems by coordination with oligopyridines and varying counterions. Indeed, D. Pucci *et al* reported previously the synthesis of several thermotropic Ag(I) complexes, built up using differently functionalized N,N-donor ligands and counterions, that exhibited lamellar or columnar 'soft' organizations with different symmetries.[10] Herein, we report the synthesis and characterization of new carboxylate ionic N,N- coordinated Ag(I) complexes, in which the length of the counterion has been varied (complexes **1-3** in Figure 1). Moreover, the choice of the hydroxyl substituents on the bipyridine ligand is related to their potential ability to help in the formation of solvate species and then to form networks of intermolecular interactions via hydrogen bonds.[11]

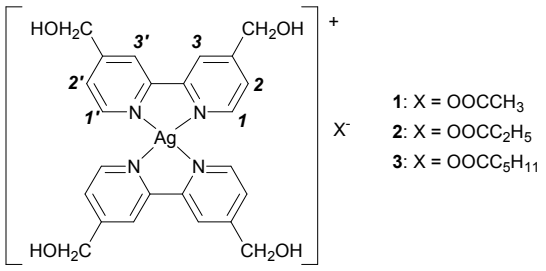

Figure 1. Chemical structures of the silver(I) complexes **1**, **2** and **3**.

The ability of these silver(I) complexes to organize into columnar structures is highlighted in the solid crystalline state, by means of single crystal X-ray analysis performed on complex **1**.

These complexes spontaneously self-assemble in water into LCLC phases, characterized by their phase diagram completely resolved by polarized optical microscopy (POM) and X-Ray powder diffraction techniques. Cryo-TEM experiments have also been carried out in order to directly reveal the chromonic nature at a suitable water concentration.[12] Furthermore, the LCLC phases have been aligned between two polymer covered glasses, following a method already reported in the literature[6i] and showing transient twisted periodical stripe structures, a sign of elastic anisotropy.

Results and discussion

Synthesis and characterization

For the synthesis of the Ag(I) complexes **1-3**, the ligand 4,4'-bis(hydroxymethyl)-2,2'-bipyridine (bpy-OH) was previously prepared according to the method reported in literature.[13] The ligand was further reacted with half equivalent of AgX, X= CH_3COO, C_2H_5COO and $C_5H_{11}COO$ respectively, for 4-6 h in EtOH, under nitrogen atmosphere in a vessel protected from light. The final complexes were obtained in relative high yields as yellowish solids, after recrystallization from EtOH/Hexane. The complexes were dried for several days under high pressure vacuum.

These complexes were fully characterized and their proposed structures were confirmed by IR, ^{1}H NMR and elemental analysis. Indeed, the IR spectra of all complex show the corresponding asymmetric and symmetric stretching vibration frequencies for the carboxylate counterions at around 1560 cm^{-1} (ν_{as} (COO^-)) and at 1390 cm^{-1} (ν_{asy}(COO^-)), respectively.[14] Furthermore, the IR spectra show a large band at approx. 3400 cm^{-1}, regardless of several attempts to dry the powders, and therefore reasonably attributable to the ,2'-bipyridine $–CH_2OH$ substituents.. The presence of solvent was revealed by TGA analysis. The thermograms show loss of weight corresponding to one water molecule for all compounds (See Supporting Information, Figs. S1-S3).

The ^{1}H NMR spectra of the complexes recorded in MeOD solutions show the signals corresponding to the protons of the carboxylate counterions and the protons of the coordinated ligand, the integration being indicative of the 2:1 stoichiometry ratio.

The ionic nature was confirmed by conductivity measurements performed in MeOH solution (See Experimental Section). Indeed, the conductivity values obtained for these complexes are characteristic for univalent electrolytes.[15]

The molecular structure of **1** has been obtained by single crystal X-ray analysis performed on suitable crystals grown from very slow evaporation of a methanol solution. The ionic nature of complex **1** is finally confirmed, with the metal cation containing the Ag(I) ion in a tetra-coordination geometry bis-chelated by two bipyridine ligands (Figure 2a). The asymmetric unit is then completed by the presence of the acetate anion and two water molecules, one of which probably crystallized over the long crystallization process. Bond distances and angles around the silver ion are in good agreement with those already reported for similar complexes.[16]

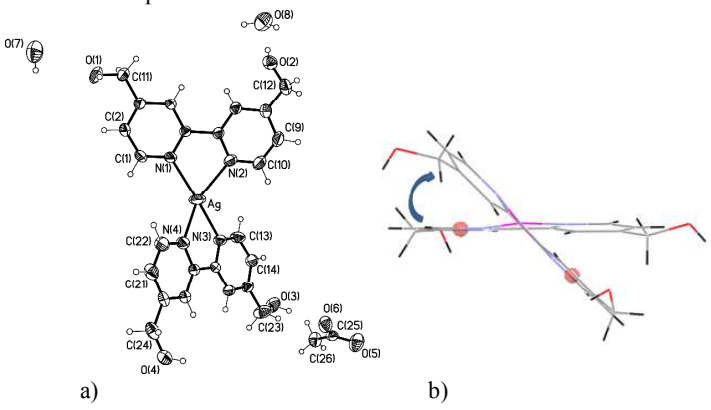

Figure 2. Perspective view of ionic complex **1** with atomic numbering scheme (ellipsoids at the 50% level) (a) and the crystallographic independent complex cation in *Λ* configuration (b).

Both coordinated bipyridine ligands deviate from planarity, showing the internal torsion angle N-C-C-N of 9.4(5) and 4.4(5)°, respectively. Generally, symmetric bis-chelate pseudo tetrahedral complexes themselves are not chiral. Nevertheless complex **1** crystallizes in the chiral orthorhombic *P*2(1)2(1)2(1) space group. The symmetry within each bipyridine is broken by means of the different mutual orientation of the $–CH_2OH$ substituents (torsion angles around the C_{arom}-C bond of: C(2)-C(3)-C(11)-O(1) 35.0(6)°, C(9)-C(8)-C(12)-O(2) 163.0(4)°, C(14)-C(15)-C(23)-O(3) 16.6(7)°, C(21)-C(20)-C(24)-O(4) 175.5(4)°), generating chirality around the metal centre. The relative orientation of the two ligands creates a helicity around the metal ion, and the absolute configuration has been properly resolved. Labelling the aromatic ring bearing the $–CH_2OH$ group with the same orientation in the two bipyridine ligands, allow to identify othe single crystallographic independent complex cation in *Λ* configuration (Figure 2b).[17]

The analysis of the intermolecular interactions existing within the asymmetric unit and in the 3D crystal packing of **1** is of particular interest for understanding the relationships between structure and LCLC properties for this class of complexes. The presence of water molecules both in the powder and in the crystalline solid state of **1** has confirmed the usefulness of the properly functionalized 2,2'-bipyridine with hydroxyl groups around the as

well as the acetate anion in the formation of water aggregates species. The presence of water molecules and the acetate anion interacting via hydrogen bonds with the hydroxyl groups at the periphery of the metal containing cation, generates the formation of cation dimeric repeating units despite the potential electrostatic repulsion (Figure 3).

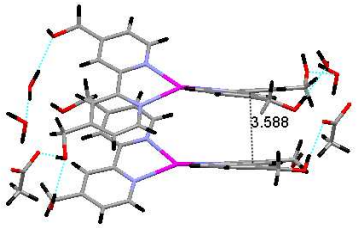

Figure 3. View of the repeating unit of metal containing cations of complex **1** within columns showing the shortest π-π stacking distance and external hydrogen bonds.

Within the dimeric unit, cations interact through aromatic π-π stacking interactions with distance of about 3.6 Å (defined as the distance between the centroid of one aromatic ring and the mean plane passing through the above aromatic coplanar ring) and the silver ions of closest cations are forced at a distance of 3.951(2) Å. The dimeric unit, regularly repeating along the *a* axis, gives rise to metal containing columns. The tight hydrogen bonding network is formed in the 3D space and the columns of metal cations are segregated between layers of acetate ions and water molecules by means of O---H hydrogen bonds type (Figure 4a).

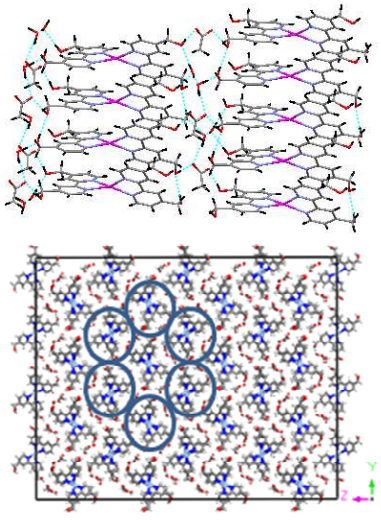

a)

b)

Figure 4. Solid state organization of complex **1** showing the formation of metal containing cation columns running along the *a* axis, held together by means of hydrogen bonds formed with acetate anions and water molecules (a) and the repetition of columns in the *bc* plane forming a 2D hexagonal structure (b).

The repetition of columns viewed down the *a* axis (in the *bc* plane) shows clearly that columns are organized in a close-packed hexagonal structure with an average intermolecular distance of about 17 Å (Figure 4b).

Phase diagram in water solutions

The phase diagram of complexes **1** and **2** were completely determined by POM and the relative type of mesophases confirmed by X-Ray Diffraction analysis. The phase diagram of complex **3** was not investigated since the nematic phase appears at a concentration above 50%wt. The decrease of the complexes hydrophilicity is related to the increase of the carboxylate counterion chain lengths.

Water solutions of complex **1** exhibit LC phases from 15%wt to 60%wt of concentration. In Figure 5, the phase diagram of complex **1** is reported with some POM pictures of the textures observed inside the cell.

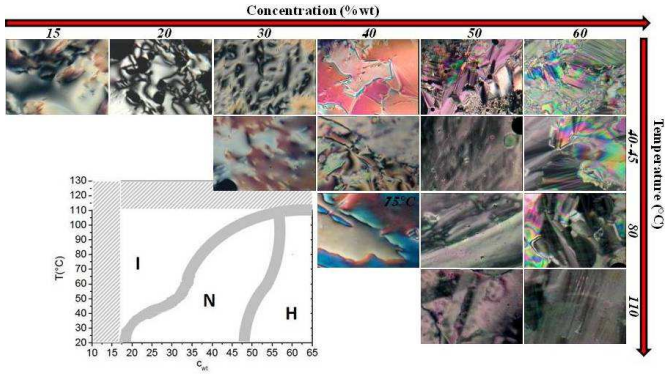

Figure 5. Phase diagram of complex **1** and POM pictures of the texture observed at different temperature and concentration, confirming the presence of LC phases

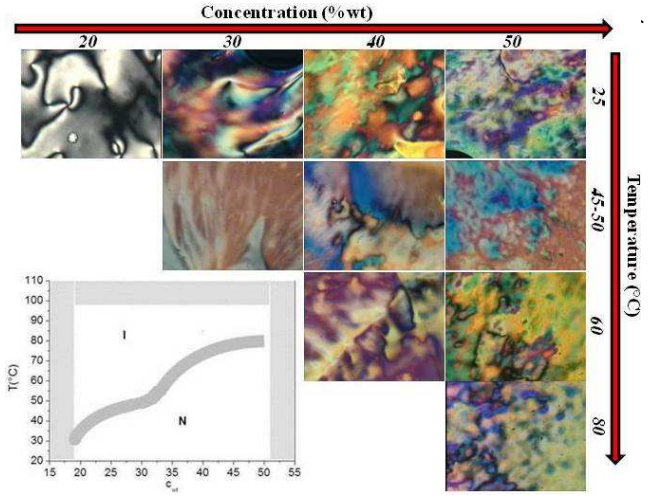

Figure 6. Phase diagram of complex **2** and POM pictures of the texture observed at different temperature and concentration, confirming the presence of LC phases

The presence of nematic and hexagonal phases at different weight concentrations together with the non amphiphilic nature of these new metal based complexes and their ability to dissolve in water forming ordered aggregates, confirm their chromonic nature.

X Ray Powder Diffraction analysis

In addition to phase diagrams and POM characterization, X-Ray powder diffraction measurements (PXRD) were done, at room temperature, on both 20%wt and 60%wt LCLCs non aligned phases of complex **1** and on 20%wt in the case of complex **2**.

In the case of complex **1**, the nematic diffuse peak in the PXRD pattern is centered at 2θ = 2.5°, corresponding to a *d* value of 35.3 Å (Figure 7).

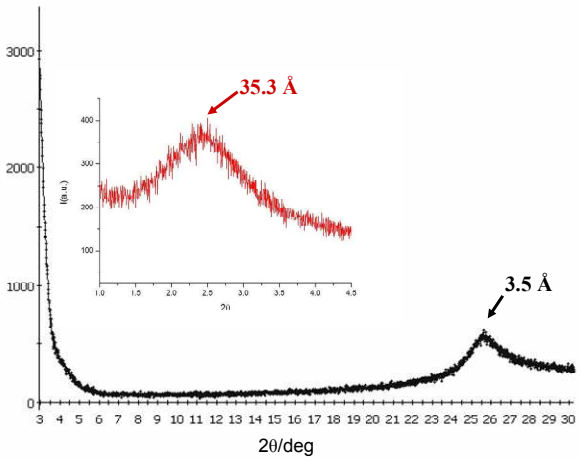

Figure 7. Complex **1** X-Ray diffraction pattern (low angle region in the inset) acquired at room temperature in the nematic phase at 20%wt concentration.

A moderately sharp reflection in the high-angle region of the PXRD pattern, is centered at 3.48 Å corresponding to the average stacking repeat distance within columns. The intensity of this high-angle reflection, sharper than the usually broad stacking repeat peak encountered in the discotic nematic phase, points towards the existence of a truly N chromonic phase.

By changing concentration, moving to 60%wt, the low angle reflection moves to 2θ = 4.88°, which corresponds to a much lower *d* value of 18.1 Å (Figure 8).

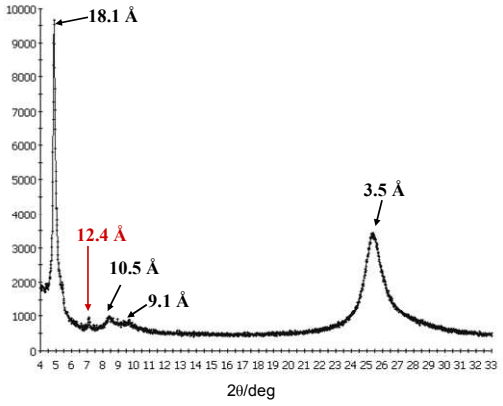

Figure 8. Complex **1** X-Ray diffraction pattern acquired at room temperature in the hexagonal phase at 60%wt concentration.

This observed *d* value reduction with the complex concentration in the water solution is consistent with a decrease of the average columns distance due to the diminished amount of "see water" in between chromonic molecules and concomitant increase of columnar organization order.[1a] The presence in the small angle region of two other reflections, together with the first one in the ratio $1:\sqrt{3}:\sqrt{4}$, are characteristic of a 2D lattice of a hexagonal columnar phase, corresponding to the indexation (*hk*) = (10), (11) and (20), with a cell parameter *a* = 20.8 Å. This value is similar to the intermolecular distance found in the close-packed hexagonal structure of the crystal phase (of about 17 Å) indicating that the hexagonal arrangement in the mesophase is obtained from the crystalline solid state through decorrelation between columns with maintenance of the intra columns interactions. Indeed, the major feature in PXRD pattern of **1** of the presence of a chromonic M phase is a sharp high-angle reflection corresponding to the stacking repeat distance of 3.51 Å. This value is found to be slightly larger than the stacking repeat distance of 3.40 Å, usually reported for organic chromonic molecules. This increase is fundamentally due to the stacking within columns of non planar molecules, aggregated through aromatic interactions between facing bipyridine fragments and consistent with the aromatic π-π stacking distance of about 3.6 Å found in the crystalline solid state.

Furthermore, the peak centred at 12.4 Å is due to some polymorphic crystalline microdomains remained underneath the the LCLC phase, as confirmed when the liquid crystalline pattern is compared with the PXRD pattern of the crystalline powder of complex **1** (See S4 in ESI).[18]

At room temperature, the PXRD pattern of complex **2** at 20% wt in water, shows at low angle a nematic peak at 2θ = 2.3°, corresponding to a *d* value of 38.4 Å (see figure S5 in ESI). This increase of the nematic *d*-spacing when compared with the one of complex **1** recorded in the same conditions should be related to the increase of the molecular length, i.e. the increase of the carboxylate counterion chain length.

Cryo-TEM analysis

Cryo-TEM analysis carried out on complex **1** solution in its nematic phase (20%wt), directly demonstrate the assembly of the molecules into columnar aggregates and the nematic arrangement of the aggregates. Figs. 9a and 9b show typical side-view (corresponding to a planar orientation of the columns with the electron beam perpendicular to the LC film) and top-view (a homeotropic orientation) of the aggregates, respectively. The aggregates are represented by the dark stripes (Fig. 9a) and dots (Fig. 9b).[11] The length of the aggregates mostly varies between 10 nm and 60 nm, measured from the side-views by assuming a planar orientation. Fig. 9a also reveals that the elongated aggregates are oriented along roughly the same direction which is also the long axis of the aggregates.

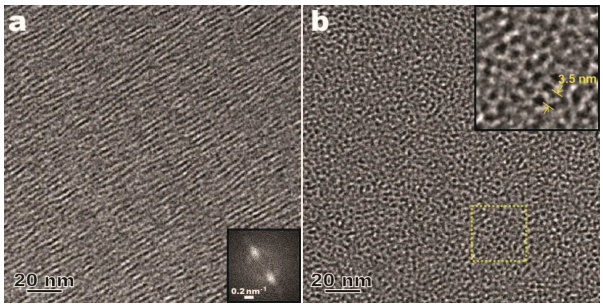

Figure 9. Cryo-TEM images of complex **1** aggregates in its nematic phase at 20%wt: side view (a) and top view (b). The inset of Fig. 9a is the corresponding FFT pattern. The inset of Fig. 9b is a magnified image of the marked area (30 nm × 30 nm) with a dashed square.

The top-views of the aggregates enable the direct observation of the distribution pattern of the aggregates in the plane perpendicular to the aggregate axis. The aggregates can arrange themselves into approximate hexagons and roughly straight lines (Fig. 9b and its inset) in local regions. However, it is quite clear that the overall distribution is random and no long-range order is formed.

The distances measured between the adjacent aggregates from the top views normally falls within the range of 3-4 nm with an average of 3.4 nm, which is in excellent agreement with the XRD result (35.3 Å). The ones measured from the side views are slightly smaller due the projection effect and have an average of ~3 nm. The fast Fourier transform (FFT) pattern in Fig. 9a shows two major diffused bright spots which are also elongated perpendicular to the aggregate axis. This indicates a rather largely varying distance between the aggregates and a slightly changing aggregate orientation. The above results clearly confirm that the 20%wt complex **1** solution has a nematic structure. It should be mentioned that currently it is still challenging for us to carry out cryo-TEM observation on highly viscous LCLCs (e.g., 60%wt complex 1), as discussed in Ref. 12.

Alignment

The alignment of LCLCs phases was carried out confining complexes **1** and **2** between two properly treated surfaces. As reported in a previous work, it is possible to align chromonic liquid crystal phases by means of polymeric substrates characterized by different surface energies.[6i] A high surface energy (Polymethyil-methacrylate - PMMA) and a low surface energy (Cytop) materials were used in this work (see Experimental Section for details).

Just after filling, the nematic phase of complex **1** (20%wt) confined between PMMA treated glasses, shows textures characterized by a coexistence of degenerate planar alignment and homeotropic anchoring. With time, the degenerate planar anchoring (Figs 10a-c) evolves in an ordered structure, characterized by stripes, disappearing after about 60-70 minutes in favor of stable homeotropic anchoring (confirmed by Maltese cross in conoscopy). The hexagonal phase, instead, shows immediately the homeotropic anchoring (Figure 10d).

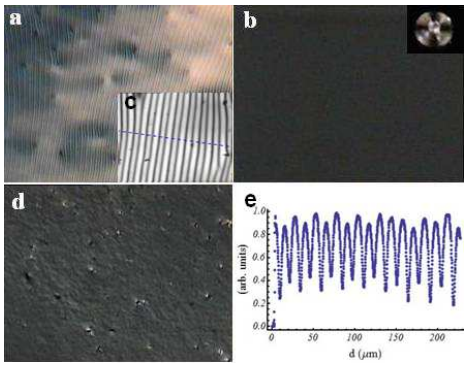

Figure 10. POM images of nematic phase (a,b,c) and hexagonal phase (d) of complex **1** confined between PMMA treated glasses. (a,b,d) are acquired using a 5x objective, while (c) using a 20x objective. e) line profile highlighting the periodicity of the stripes observed in (c). The mean pitch measured is of 25 μm, with a modulation in the middle at about 13 μm.

Recently, J. Jeong *et al* reported the presence of transient stripes in sunset yellow nematic LCLCs phase when confined between parylene coated glasses.[19] The transient stripes reported are, in average, aligned parallel to the direction of the initial flow, inducing a planar alignment. The authors model was further confirmed by compensator and POM measurements. Even if a different polymer was used in our case, the stripes observed are transient too, and disappear in favor of the homeotropic configuration after about 1 hour and half. It is possible to re-induce stripes formation by heating up the cell to 60°C and slowly cooling down the system, until the homeotropic alignment is reached again. In order to evaluate the stripes periodicity, the images were analyzed with a home-made program written in Mathematica, obtaining a periodicity of about 25μm, with a modulation in the middle at about 13μm.

The stripes were investigated crossing and uncrossing polarizer and analyzer, and inserting in the optical path a tilting compensator (5λ) confirming the twisting nature of the periodicity observed (Figure 11).[19]

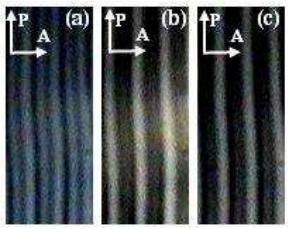

Figure 11. Optical microscopy images of the stripe textures under crossed polarizers. White arrows represent the directions of the input polarizer (P) and the analyzer (a). In b) and c) the tilting compensator is inserted in the optical path.

A detailed analysis is reported in Figure 11; all images reported were acquired in the same region using a 20x objective. The direction of analyzer and polarizer are reported in the pictures. The stripes are not clearly visible when polarizer and analyzer are parallel or when only one polarizing plate is present. The sketch of the model proposed by J. Jeong *et al.*[19] and reported for clarity in Figure S6 in ESI, may be taken into consideration.

These stripes appear as a balance of confining surface energy, self assembly properties and LCLC elastic constants anisotropy: the twist constant is at least one order of magnitude less than the splay and bend ones; the cell thickness plays as well an important role in stripes dimension. The tilting compensator rotated in both directions compensates alternatively the stripes doubling their spacing and confirming their twisted nature. The same experiments were done using LC solutions of complex **2** at 20 %wt and no stripes were observed (data not reported).

Different scenario is observed for the "low surface energy material" used as alignment layer. Indeed, when Complex **1** (i.e. 20%wt) is confined between Cytop treated glasses, an initial perfect planar alignment is observed, that rapidly disappear in favor of well ordered stripes, that cover the whole cell. After 3 hours, the molecules reorient in the whole cell, reaching a homeotropic alignment. The stripes pitch is in this case about 14 μm. If an external stress is applied to the cell, the planar alignment could be reproduced and follows the same evolution in time described above (Figure S7 in ESI). A similar behavior but with an initial quasi-perfect planar alignment with some characteristic defects (Schlieren texture) is observed for complex **2** but in this case, the periodicity of the stripes is doubled (25μm) (Figure S8 in ESI).

From the optical observation reported here, a discotic-like behaviour for the compounds may be suggested. A planar alignment of the LC phases, for both complexes, was achieved temporarily only with highly hydrophobic surfaces even if the final configuration, is always the homeotropic one. It seems that highly hydrophobic substrates are able to disrupt in some way the aggregates forming the LC phases, allowing an initial planar (complex **1**) and quasi planar (complex **2**) alignment, that is lost in favor of a more stable hometropic configuration. This means that in the competition between the alignment imposed by the substrates and the forces that bond the aggregates together, the π-π stacking between the disks win the anchoring energy.

Conclusions

The synthesis and characterization of the ionic Ag(I) complexes **1**, **2** and **3**, having aliphatic carboxylate counterions with different chain lengths are reported. The single crystal X ray structure analysis of complex **1** has confirmed its ionic nature as well as the great affinity to aggregate in water. The presence of co-crystallized water molecules and the acetate anion interacting via hydrogen bonds with the hydroxyl groups at the periphery of the metal containing cation, generates the formation of cation dimeric repeating units despite of the potential electrostatic repulsion. In the 3D space, cations organize themselves into columns along the *a* axis and the metal containing columns are imbibed between layers of strongly interacting water molecules and acetate anions. The cations stack into columns held together by π-π interactions helped by hydrogen bonding with the acetate counterions and water molecules. The repetition of columns in the *bc* plane shows clearly their organization in a close-packed hexagonal structure with an average intermolecular distance of about 17 Å.

Even if the structural features of these new Ag(I) complexes does not fit the characteristic class of molecules forming LCLC phases, complexes **1** and **2** spontaneously self-assembly into nematic and hexagonal chromonic phases in water.

The suppression of the hexagonal phase in complexes **2** and **3** and also the appearance of the nematic organization at higher concentration with respect to complex **1** (particularly in the case of complex **3**), is clearly related to the counterion. With the increasing of the counterion chain length, its facility to be involved in hydrogen bonding with water molecules should be inhibited, probably blocking the formation of the cation dimeric repeating units and favoring their electrostatic repulsions.

Therefore, the characterization of the LCLC formed phases has been performed on complexes **1** and **2** in water solution at different concentrations.

The phase diagram of complexes **1** and **2**, completely resolved by POM, has firstly indicated the formation of nematic and hexagonal phases in the case of complex **1** at 20% wt and 60%wt of concentration, while only nematic aggregation is observed in the case of complex **2**. PXRD measurements performed at the various concentration have confirmed the formation of chromonic phases by dispersion of complexes **1** and **2** in water. Both nematic and hexagonal phases in the case of complex **1**, have shown in the wide angle region of the PXRD pattern a reflection centered at about 3.5 Å, whose intensity and sharpness points towards the existence of truly N and M chromonic phases. The same feature has confirmed in the case of complex **2** in the only observed N phase. Moreover, the hexagonal cell parameter of 20.8 Å calculated in the M mesophase in the case of **1**, is in agreement to the intermolecular distance found in its close-packed hexagonal organization in the crystalline solid state (of about 17 Å), indicating that the mesophase is most probably arising from the crystalline phase through decorrelation between columns with maintenance of the intra column interactions.

The direct cryo-TEM observation of the 20%wt solution of complex **1** have revealed the top- and side-views of elongated column, and confirm the self-assembly of the molecules into columnar aggregates. The aggregates are normally 10-60 nm long and are preferentially oriented along their long axis. The distribution of the aggregates is rather random and has no long-range order in the plane perpendicular to the aggregate axis, consistent with a nematic nature. In addition, the distance between the aggregate axis measured from the cryo-TEM results matches closely the XRD result. Based on the cryo-TEM and XRD results, it is reasonable to assume a hexagonal lattice for higher concentration solutions, though a direct cryo-TEM observation is still not available.

In addition, the LCLC phases of both complexes were aligned between two polymer covered glasses showing transient twisted periodical stripe structures that are a sign of elastic anisotropy, proving their potential for applications in optical devices or biosensing.

In conclusion, the synthesis and characterization of unconventional Ag(I) chromonic complexes have been reported. Most probably these complexes assemble in water forming LCLC phases due to the presence of suitable building blocks, such as the right anions and N,N-coordinated ligand substituents, as well as the metal ion. A route for future synthesis of metal based chromonic compounds has been highlighted, as well as the

opening to a new branch of applications in biocompatible devices.

Experimental

Materials and measurements

All commercially available starting materials were used as received without further purification.

Instrumentation

The ^{1}H NMR spectra were recorded on a BrukerAvance AC-300 spectrometer in MeOD solution, using tetramethylsilane (TMS) as internal standar. Elemental analyses (CHN) were performed with Perkin Elmer 2400 microanalyzer by the Microanalytical Laboratory at the University of Calabria. Infrared spectra (KBr) were recorded on a Spectrum One FT-IR Perkin Elmer spectrometer. A Perkin-Elmer Lambda 900 spectrophotometer was used to record absortion spectra complexes on water solutions. AInoLab Cond Level 1-720 conductometer equipped with LR 325/001 immersion cell was used to conductivity measures. The thermal stability was measured on a Perkin-Elmer Termogravimetric Analyser Pyris 6 TGA. Bright field, polarized optical microscopy (POM) images and conoscopy images were collected using a microscope (Zeiss) with a 5x, 20x objective or 100x objective, respectively. The calibration of the microscope hot stage was performed by checking the transition temperatures of the E7 liquid crystal. The samples were rotated on a circular stage located between a polarizer and an analyzer. Most images were taken with a colour CCD camera under polychromatic illumination.

X-ray Crystallography

X-ray data for **1** were collected at room temperature on a Bruker-Nonius X8 Apex CCD area detector equipped with graphite monochromator and Mo Kα radiation (λ = 0.71073 Å). Data were processed through the SAINT[20] reduction and SADABS[21] absorption software. The structures were solved by standard Patterson methods through the SHELXTL-NT[22] structure determination package and refined by full-matrix least-squares based on F^2. In general, all non-hydrogen atoms were refined anisotropically and hydrogen atoms were included as idealized atoms riding on the respective carbon atoms with C-H bond lengths appropriate to the carbon atom hybridization. Hydrogen atoms of the co-crystallized water molecules have been included in calculated positions and restrained bond distances and angles have been used.

Details of data and structure refinements are given in Table 1. CCDC 1017854 (**1**) contains the supplementary crystallographic data for this paper. These data can be obtained free of charge from The Cambridge Crystallographic Data Centre via www.ccdc.cam.ac.uk/data_request/cif.

Powder X-ray diffraction

The powder X-ray diffraction patterns of complex 1 in its hexagonal phase and nematic phase in the wide angle region as well as in the solid state were obtained at room temperature by using a Bruker D2 PHASER Diffraction System equipped with 1D high speed solid state LinxEye detector and Cu-Kα radiation (λ = 1.54056 Å). Measurements were performed by placing samples on a zero background sample holder with protection for solvent evaporation along the measurements.

The X ray pattern of complexes **1** and **2** in their nematic phase at low angle were obtained at room temperature using a D8 Discover, Bruker-AXS with Cu-Kα radiation (λ = 1.5418 Å). The LC solutions were hosted in a glass capillary (Mark tubes, Hilgenberg, 80 mm length, outside diameter 0.8 mm or 1 mm and wall thickness 0.1 mm) placed in a home-made sample holder.

Cryo-TEM measurements

The cryo-TEM observation was carried out using a FEI Tecnai F20 microscope (200 KV) equipped with an anti-contaminator, a low-dose operation mode, and a Gatan UltraScan 4000 CCD camera. To prepare cryo-TEM specimens, we employ a FEI Vitrobot (environmental chamber set to 22 °C) to plunge-freeze liquid crystal thin films supported by holey carbon coated grids. Liquid ethane was used as the cryogen in the rapid cooling process to ensure the preservation of the native structure. The vitrified LC specimens were then mounted on a Gatan 626.DH cryo-holder and transferred into the TEM. During the whole specimen transfer and TEM observation process, the TEM specimen was kept at temperatures below -170°C. The TEM images shown here were all taken from the electron-transparent areas suspended in the holes of the supporting carbon films.

Synthesis of complexes 1-3

[(Bpy-OH)$_2$Ag][CH$_3$COO]·H$_2$O, 1. To a solution of 2 eq. of bpy-OH (100 mg, 0.46 mmol) in EtOH was added 1 eq. of $AgOOCCH_3$ (30 mg, 0.23 mmol). The solution was stirred 4 hours under nitrogen and darkness. The solution was filtered, washed with EtOH, concentrate under reduced pressure and recrystallized from n-hexane. (203 mg, 72% yield). Mp 182º C. IR (ν_{max}/cm^{-1}: 3369 (OH), 2920-2818 (CH), 1602 (C-C), 1560(ν_{asy} C=O), 1407 (ν_{sym} C=O). ^{1}H NMR (300MHz, MeOD): δ_H 8.58 (d, 4H, *J*(H-H)= 5.07 Hz, $H_{1,1'}$), 8.39 (s, 4H, $H_{3,3'}$), 7.58 (d, 4H, *J*(H-H)= 4.66 Hz, $H_{2,2'}$), 4.91 (s, 8H, CH_2), 1.89(s, 3H, CH_3). Anal. Calc. for $C_{26}H_{29}AgN_4O_7$ (671.40 g/mol): C, 50.58; H, 4.73; N, 9.07. Found: C, 50.41; H, 4.57; N, 9.14%. UV-vis (H_2O) λ_{max} (ε, $M^{-1}\cdot cm^{-1}$): 235nm (61699), 281nm (72087). Λ_{MeOH}= 82.72 $\Omega^{-1}\cdot cm^2\cdot mol^{-1}$.

[(Bpy-OH)$_2$Ag][CH$_3$CH$_2$COO]·H$_2$O, 2. To a solution of 2 eq. of bpy-OH (100 mg, 0.46 mmol) in EtOH was added 1 eq. of $AgOOCCH_2CH_3$ (41.6 mg, 0.23 mmol). The solution was stirred 4 hours under nitrogen and darkness. The solution was filtered, washed with EtOH, concentrate under reduced pressure and recrystallized from n-hexane. (176 mg, 63% yield). Mp 171º C(dec.). IR (ν_{max}/cm^{-1}: 3370 (OH), 2884-2833 (CH), 1603 (C-C), 1562 (ν_{asy} C=O), 1407 (ν_{sym} C=O). ^{1}H NMR (300MHz, MeOD): δ_H 8.58 (d, 4H, *J*(H-H)= 5.1 Hz, $H_{1,1'}$), 8.38 (s, 4H, $H_{3,3'}$), 7.58 (d, 4H, *J*(H-H)= 4.6 Hz, $H_{2,2'}$), 4.83 (s, 8H, CH_2), 2.15 (q, 2H, *J*(H-H)=22.86, H_a), 1.08 (s, 3H, CH_3). Anal. Calc. for $C_{27}H_{31}AgN_4O_7$ (631.43 g/mol): C, 51.36; H, 4.95; N, 8.87. Found: C, 51.26; H, 5.14; N, 8.86%. UV-vis (H_2O) λ_{max} (ε, M$^-$

$^{1}\cdot cm^{-1}$): 234nm (13608), 282nm (14822). Λ_{MeOH}= 87.83 $\Omega^{-1}\cdot cm^{2}\cdot mol^{-1}$.

Table 1 Details of data collection and structure refinements for complex **1**

	1
formula	$C_{26}H_{31}AgN_4O_8$
Mr	635.42
crystal size [mm]	0.32 x 0.18 x 0.12
crystal system	Orthorhombic
space group	$P2_12_12_1$
a [Å]	7.7993(4)
b [Å]	16.4226(8)
c [Å]	20.2988(11)
α [°]	90
β [°]	90
γ [°]	90
V [Å^3]	2600.0(2)
Z	4
ρ cald [gcm^{-3}]	1.623
μ [cm^{-1}]	0.833
θ range [°]	1.59-24.94
data collected	48505
unique data, R_{int}	4542, 0.0360
obs. data [$I > 2\sigma(I)$]	4100
no. parameters	364
Flack parameter	0.00(3)
R_1 [obs. data]	0.0335
wR_2 [all data]	0.0996
GOF	1.106

[(Bpy-OH)$_2$Ag][CH$_3$CH$_2$CH$_2$CH$_2$CH$_2$COO]·H$_2$O, 3. To a solution of 2 eq. of Bpy-OH (100 mg, 0.46 mmol) in EtOH was added 1 eq. of AgOOCCH$_2$CH$_2$CH$_2$CH$_2$CH$_3$ (51 mg, 0.23 mmol). The solution was stirred 6 hours under nitrogen and darkness. The solution was filtered, washed with EtOH, concentrate under reduced pressure and recrystallized from n-hexane. (108 mg, 71% yield). Mp 139º C(dec). IR (ν_{max}/cm^{-1}: 3369 (OH), 1604 (C-C), 1564 (ν_{asy} C=O), 1408 (ν_{sym} C=O). ^{1}H NMR (300MHz, MeOD): δ_H8.57 (d, 4H, *J*(H-H)= 5.25 Hz, $H_{1,1'}$), 8.38 (s, 4H, $H_{3,3'}$), 7.57 (d, 4H, *J*(H-H)= 6.53 Hz, $H_{2,2'}$), 4.82 (s, 8H, CH_2), 2.13 (t, 2H, *J*(H-H)=7.8, H_a), 1.58 (q), 2H, *J*(H-H)=7.52, H_b), 1.31 (m, 4H, $H_{c,d}$),0.88 (t, 3H, *J*(H-H)=6.91,CH_3). Anal. Calc. for $C_{30}H_{37}AgN_4O_7$ (673.51 g/mol): C, 53.50; H, 5.54; N, 8.32. Found: C, 53.38; H, 5.51; N, 8.45%. UV-vis (H_2O) λ_{max} (ε, $M^{-1}\cdot cm^{-1}$): 235nm (16008), 283nm (19439). Λ_{MeOH}= 59.49 $\Omega^{-1}\cdot cm^{2}\cdot mol^{-1}$.

Mesophases and cells preparation

Liquid crystal solutions of both compounds were prepared by dissolving an amount of complex **1** and **2** in pure distilled water (Millipore, 18MΩ cm) in a range of concentrations between 15%wt and 60%wt. Glass slides used for the preparation of the cells were obtained from Pearl, China. They were cleaned in a NaOH bath, sonicated for 15 minutes and rinsed several times with Millipore water before drying them under a heat flow. For the phase diagram studies, we used bare glasses for the preparation of the cells, while for the alignment studies, the glasses were pre-treated covering them with polymeric films, in order to obtain planar or homeotropic alignment of the LCLCs solutions. Polymethyil-methacrylate (PMMA) was purchased from Sigma Aldrich, while Cytop, a highly transparent fluoropolymer, has been obtained from Asahi Glass. Polymeric thin films were prepared by spin coating technique, at 3000rpm, using a spin coater from Calctec (Italy), followed by an appropriate thermal treatment. PMMA treated glasses, after cooling down, were rubbed using a custom built machine, with a rotating velvet cloth.

Cells were assembled using two glasses with the same surface treatment and 12μm mylar stripes as spacers, hence they were filled with the LC solution in isotropic phase and sealed by an epoxy glue, in order to avoid water evaporation. After filling, each cell was slowly cooled down and observed by polarized optical microscopy (POM). Each cell has been subjected to a temperature cycle in order to test the sealing. We focused our attention on complex **1** and **2**, because complex **3** presents nematic phase only at very high concentration (50%wt).

Acknowledgements

Financial support received from the Ministero dell'Istruzione, dell'Università e della Ricerca (MIUR) through the Centro di Eccellenza CEMIF.CAL (CLAB01TYEF), from by the Italian PRIN founding n. 2006038447 and by the European Community's Seventh Framework Program (FP7 2007-2013), through MATERIA project (PONa3_00370) is gratefully acknowledged. The TEM results were taken at the TEM Lab of the Liquid Crystal Institute (LCI) at Kent State University, supported by the Ohio Research Scholars Program *Research Cluster on Surfaces in Advanced Materials*. M.G. thanks the LCI Characterization Facility for the support of his TEM study. E.I.S. further acknowledges the European Union and Regione Calabria (Fondo Sociale Europeo, POR Calabria FSE 2007/2013) for partial funding.

Notes and references

[a] *(Daniela Pucci, Barbara Sanz Mendiguchia, Elisabeta Ildyko Szerb, Mauro Ghedini, Alessandra Crispini)* Centro di Eccellenza CEMIF.CAL, LASCAMM CR-INSTM and Laboratorio Regionale Licryl, CNR-INFM, Dipartimento di Chimica e Tecnologie Chimiche, Università della Calabria, 87030 Arcavacata di Rende (CS, Italy); *E-mail: a.crispini@unical.it; b (Caterina Maria Tone),* Physics Department, University of Calabria, Via P. Bucci 33B, 87036 Arcavacata di Rende (CS), Italy; *E-mail: caterina.tone@fis.unical.it*; [c] *(Federica Ciuchi),* IPCF-CNR UOS Cosenza, c/o Physics Department, University of Calabria, Via P. Bucci,33B, 87036 Arcavacata di Rende,

(CS) Italy; *E-mail: federica.ciuchi@cnr.it;* [d]*(Min Gao)* Liquid Crystal Insitute and Chemical Physics Interdisciplinary Program, Kent State University,Kent, OH 44242, USA*; E-mail: mgao@kent.edu* .

† Dedicated to the late Prof. Daniela Pucci

§ Electronic supplementary information (ESI) available: Phase diagram Tables of **1** and **2**; TGA traces of **1**, **2**, **3** complexes; solid state PXRD pattern of **1**; low angle PXRD patter of complex **2** in its nematic phase; POM images of the nematic phase of complex **1** and **2** aligned between Cytop treated glasses; Simplified sketch of LC director inside stripes; CCDC 1017854 for **1**.

1 (*a*) J. Lydon, in *Handbook of Liquid Crystals*, ed. D. Demus, J. Goodby, G. W. Gray, H.-W. Spiess and V. Vill, Wiley-VCH, Weinheim, 1998, vol. 2B, p. 98; (*b*) J. Jydon, *Curr. Opin. Colloid Interface Sci*. 2004, **8**, 480-490; (*c*) J. Lydon, *J. Mater. Chem.,* 2010, **20**, 10071-10099; (*d*) J. Lydon, *Liq. Cryst*., 2011, **38**, 1663-1681.

2 S. Tam-Chang and L. Huang, *Chem. Commun*., 2008, 1957-1967.

3 (*a*) S.V. Shiyanovskii, O. D. Lavrentovich, T. Scneider, T. Ishikawa, I. I. Smalyukh, C. J. Woolverton, G. D. Niehaus and K. J. Doane, *Mol. Cryst. Liq. Cryst*. 2005, **434**, 259/[587]-270/[598]; (*b*) S. L. Helfinstine, O. D. Lavrentovich and C. J. Woolverton, *Letters in Appl. Microbiology*, 2006, **43**, 27-32; (*c*) V. G. Nazarenko, O. P. Boiko, M. I. Anisimov, A. K. Kadaschuk, Yu. A. Nastishin, A. B. Golovin and O. D. Lavrentovich, *Appl. Phys. Lett*., 2010, **97**, 263305-3.

4 T. K. Atwood, J. E. Lydon, C. Hall and G. J. T. Tiddy, *Liq. Cryst*., 1990, **7**, 657-668.

5 (*a*) P. K. Maiti, Y. Lansac, M. A. Glaser and N. A. Clark, *Liq. Cryst*., 2002, **29**, 619-626; (*b*) M. R. Tomasik and P. J. Collins, *J. Phys. Chem. B*, 2008, **112**, 9883-9889; (*c*) P. J. Collings, A. J. Dickinson and E. C. Smith, *Liq. Cryst*. 2010, **37**, 701-710.

6 (*a*) I. K. Iverson, and S. Tam-Chang, *J. Am. Chem. Soc*., 1999, **121**, 5801-5802; (*b*) D. Matsunaga, T. Tamaki. H. Akiyama and K. Ichimura, *Adv. Mat.,* 2002, **14**, 1477; (*c*) I. K. Iverson, S. M. Casey, W. Seo and S. Tam-Chang, *Lagmuir*, 2002, **18**, 3510-3516; (*d*) T. Fujiwara and K. Ichimura, *J. Mater. Chem*., 2002, **12**, 3387-3391; (*e*) Y. A. Nastishin, H. Liu, T. Scheneider, V. Nazaremko, R. Vasyuta, S. V. Shiyanovskii and O. D. Lavrentovich, *Phys. Rev. E*, 2005, **72**, 041711; (*f*) United States Patent 7, 294, 370, Lavrentovich *et al.* November 13 (2007); (*g*) V. G. Nazarenko, O.P. Boiko, H. S. Park, O. M. Brodyn, M. M. Omelchenko, L. Tortora, Y. A. Nastishin and O. D. Lavrentovich, *Phys. Rev. Lett*., 2010, **105**, 017801; (*h*) K. A. Simon, E. A. Burton, F. Cheng, N. Varghese, E. R. Falcone, L. Wu and Y. Luk, *Chem. Mat.*, 2010, **22**, 2434-2441; (*i*) C. M. Tone, M. P. De Santo, M. G. Buonomenna, G. Golemme and F. Ciuchi, *Soft Matter*., 2012, **8**, 8478-8482.

7 (*a*) W. Lu, Y. Chen, V. A. L. Roy, S. Sin-Yin Chui and C. Che, *Angew. Chem. Int*., 2009, **48**, 7621-7625; (*b*) J. E. Halls, R. W. Bourne, K. J. Wright, L. I. Partington, M. G. Tamba, Y. Z. T. Ramakrishnappa, G. H. Mehl, S. M. Kelly and J. D. Wadhawan, *Electrochem. Commun.*, 2012, **19**, 50-54; (*c*) Y. J. Yadav, B. Heinrich, G. de Luca, A. Talarico, T. F. Mastropietro, M. Ghedini, B. Donnio and E. I. Szerb, *Adv. Optical Mater*., 2013, **1**, 844-854, (d) X.-S. Xiao, W. Lu and C.-M. Che, *Chem. Sci.* 2014, **5**, 2482-2488.

8 B. Donnio, *Curr. Opin. Colloid Interface Sci*. 2002, **7**, 371-394.

9 (*a*) *Metallomesogens, Synthesis, Properties and Applications*, ed. J. L. Serrano, VCH, Weinheim, Germany, 1996; (*b*) B. Donnio and Duncan W. Bruce in *Liquid Crystals II, Structure and Bonding*, Springer, Berlin Heidelberg, Volume 95, 1999, 193-247; (*c*) B. Donnio, D. Guillon, R. Deschenaux and D. W. Bruce in *Comprehensive Coordination Chemistry II*, ed.: J. A. McCleverty and T. J. Meyer, Elsevier, Oxford, UK, 2003, 357–627.

10 (*a*) D. Pucci, G. Barberio, A. Bellusci, A. Crispini, M. La Deda, M. Ghedini and E. I. Szerb, *Eur. J. Inorg. Chem*. 2005, 2457-2463; (*b*) D. Pucci, G. Barberio, A. Bellusci, A. Crispini, M. Ghedini and E. I. Szerb, *Mol. Cryst. Liq. Cryst.* 2005, **441**, 251-260; (*c*) D. Pucci, G. Barberio, A. Bellusci, A. Crispini, B. Donnio, L. Giorgini. M. Ghedini and E. I. Szerb, C*hem. Eur. J*. 2006, **12**, 6738-6747; (*d*) A. Bellusci, M. Ghedini, L. Giorgini, F. Gozzo, E. I. Szerb, A. Crispini and D. Pucci, *Dalton Trans*. 2009, 7381-7389; (*e*) D. Pucci, A. Crispini, M. Ghedini, E. I. Szerb and M. La Deda, *Dalton Trans*. 2011, **40**, 4614-4622; (f) E. I. Szerb, D. Pucci, A. Crispini and M. La Deda, *Mol. Cryst. Liq. Cryst*. 2013, **573**, 34-45.

11 B. Sanz Mendiguchia, D. Pucci, T.F. Mastropietro, M. Ghedini and A. Crispini, *Dalton Trans*. 2013, **42**, 6768-6774.

12 M. Gao, Y.-K. Kim, C. Zhang, V. Borshch, S. Zhou, H.-S. Park, A. Jákli, O. D. Lavrentovich, M.-G. Tamba, A. Kohlmeier, G. H. Mehl, W. Weissflog, D. Studer, B. Zuber, H. Gnägi and F. Lin, *Microscopy Research and Technique,* 2014*, in press*.

13 G.Will, G. Boschloo, S. Nagaraja Rao and D. Fitzmaurice, *J. Phys. Chem*. B, 1999, **103**, 8067-8079.

14 N. W. Alcock and V. M. Tracy, *J. C. S. Dalton*, 1976, 2243-2246.

15 W. J. Geary, *Coord. Chem. Rev*. 1971, **7**, 81.

16 A. Bellusci, A. Crispini, D. Pucci, E. I. Szerb and M. Ghedini, *Cryst. Growth & Des*., 2008, **8**, 3114-3122.

17 U. Knof and Alex von Zelewsky, *Angew. Chem. Int. Ed.*, 1999, **38**, 302- 322.

18 L. Wu, J. Lal, K. A. Simon, E. A. Burton and Y.-Y. Luk, *J. Am. Chem. Soc*. 2009, **131**, 7430-7443.

19 J. Jeong, G. Han, A. T. Charlie Johnson, P. J. Collings,T.C. Lubensky and A.G. Yodh, *Langmuir*, 2014, **30**, 2914.

20 *SAINT*, Version 6.45 Copyright 2003, Bruker Analytical X-ray Systems Inc.

21 G.M. Sheldrick, *SADABS*. Version 2.10, Bruker AXS Inc., Madison, WI, USA, 2003

22 *SHELXTL-NT*, Version 5.1 Copyright (c) 1999, Bruker Analytical X-ray Systems Inc.